Journal of Applied Polymer Science

Preparation and Characterization of Supermacroporous Polyacrylamide Cryogel Beads for Biotechnological Application

Xiao-Yong Zhan, Dan-Ping Lu, Dong-Qiang Lin, Shan-Jing Yao
Department of Chemical and Biological Engineering, Zhejiang University, Hangzhou 310027, People's Republic of China
Correspondence to: S.-J. Yao (E-mail: yaosj@zju.edu.cn).

ABSTRACT: Polymer beads, particularly supermacroporous beads, play important roles in biotechnological applications, such as their application as adsorbents in bioseparation processes and used as carriers in immobilization of cells or/and enzymes. In this study, supermacroporous polyacrylamide (pAAm) based cryogel beads were prepared via an inverse suspension polymerization method at low temperature (<0°C). Standard porous beads were also prepared at room temperature for comparison. The results showed that the diameter of the beads were in the range of 50–400 μm and some irregular large pores of the beads were of 3–90 μm in diameter, which had good biocompatibility, hydrophilicity, high porosity and large connected pores. To modify the properties of these cryogel beads, cryogel beads embedded with nanoparticles of TiO_2 were also prepared. The physical properties of the composite cryogel beads with supermacroporous were characterized and the results showed an improvement in mechanical strength and stability, which indicated that these supermacroporous cryogel beads may be useful in biotechnological applications as the networks in the beads can facilitate the mass transfer of nutrients and oxygen. © 2013 Wiley Periodicals, Inc. J. Appl. Polym. Sci. 130: 3082–3089, 2013

KEYWORDS: morphology; polyamides; composites; applications; synthesis and processing

Received 3 March 2013; accepted 12 May 2013; Published online 8 June 2013
DOI: 10.1002/app.39545

INTRODUCTION

Polymer beads have unique internal structures and are widely used in many industrial areas, which have attracted more and more research interests recently. Supermacroporous polymer beads which contain well-developed porous structures have a wide range of applications like used as supporters for catalysts, immobilization of enzymes and cells, adsorptions processes, release of active substances, tissue engineering, and so forth.[1–5] The structure of supermacroporous beads can improve the diffusion of solutes through polymeric networks and the interaction of activity groups, and these beads are suitable for applications in bioseperation.[6] Moreover, the high porosity of the beads can be used to absorb large amount of water without the dissolution of the beads.[7,8]

Ideally, supermacroporous beads should be constructed from biocompatible materials, and the porogen and organic solvent used during the fabrication process should be nontoxic or completely removed afterwards. Supermacroporous beads with a diameter of 100–500 μm are most desirable in terms of cell viability, because cells leave fresh media more than a few hundred micrometers will suffer from insufficient supply of nutrients and oxygen. For the same reason, the surface pores should be widely open and all pores in the beads should be interconnected. In general, the pores in the beads should be over 20 μm in diameter to accommodate most types of applications.[9] Furthermore, the porous beads should have sufficient mechanical strength to hold, support and protect the internal of the material. Both polymeric (natural and synthetic) and inorganic materials can be used for the fabrication of porous beads. The material should be carefully selected for specific applications.[10]

Porous beads especially supermacroporous beads are preferred in medicine, cell delivery and other applications. One of the popular techniques used in porous beads preparation is by adding porogens into traditional nonporous beads and removing the porogen after the formation of the beads. Typical porogens include inorganic salts and organic solvents. For example, calcium carbonate is one of the most popular salts used as porogen. Pores are formed by mixing calcium carbonate with precursors of the beads and then removed by the hydrochloric acid.[11–16]

Recently, cryogel technology has emerged as a potential approach to produce polymeric scaffolds.[17–25] Lozinsky found that gel-like systems may be formed through appropriate regimes of freezing, storage in the frozen state and thawing.[26] Polymeric cryogels are sponge-like materials with supermacroporous structures. When cooling the solution to subzero temperature, water forms ice crystal as the porogen applied the pores sizes from several to hundreds of microns. The pores size

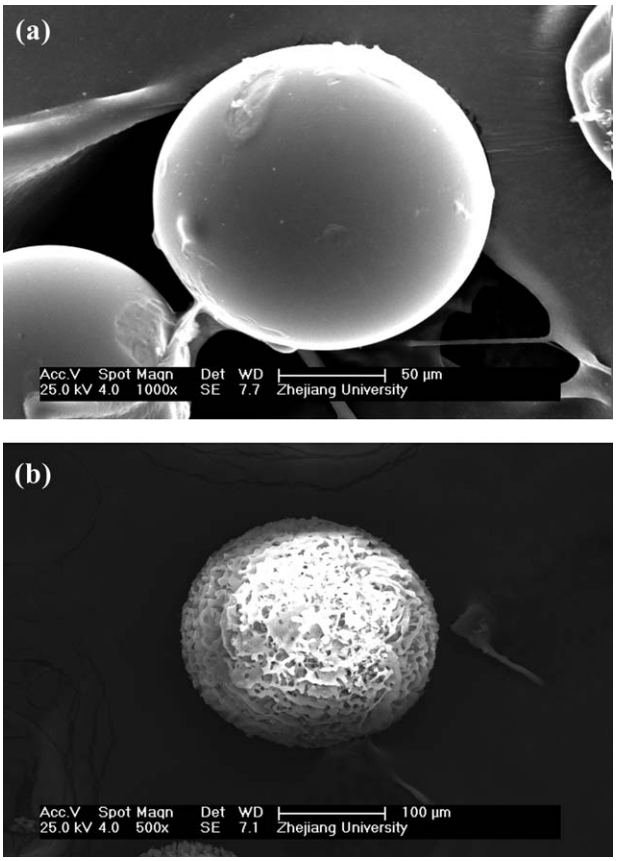

Figure 1. The morphology of the beads prepared at 20 and −12°C. (a) The morphology of nonporous pAAm beads prepared at 20°C. (b) The supermacroporous pAAm cryogel beads prepared at −12°C.

of the cryogels is depended on the gel precursors and the chemical reaction applied. For example, physically crosslinked polyvinyl alcohol (PVA) cryogels were prepared by pressed the aqueous PVA solution into liquid-jet-head where the jet is splintered into droplets by the flow of water immiscible solvent. The pore size of the beads was up to 1 μm. Another type of cryogel was produced through a free-radical polymerization reaction in an aqueous medium at subzero temperature. A typical example for such cryogels is the polyacrylamide (PAAm) cryogel. This cryogel is usually designed as monolithic, discs or sheets with pore size up to hundreds of microns.[18,27,28]

Polyacrylamide has good biological properties and is hydrophilic with good biocompatibility and stable chemical properties, and it can be easily functionalized. Polyacrylamide (pAAm)-based cryogels are a popular class of supermacroporous monoliths in biotechnology applications. It is also possible to prepare crygels in bead form with similar methods, i.e., by freezing-thawing aqueous droplets containing gel-forming monomers.[29–31] Most of these methods are convenient to operate and suitable for preparing cryogel beads used for immobilization purposes, but they also suffer from challenges such as accurately controlling of bead sizes and need relatively complex equipments. The size of the beads are often larger than 1 mm.

Nanoparticles embedded in polymer networks have great advantages in biochemical applications. For example, nano-TiO_2 plays an important role in environmental nanotechnology for its ability of resisting and decomposing bacteria, UV resistance and excellent transparency for visible lights. Nano-Fe_3O_4 with good magnetic properties embedded in polymer matrices makes the separation of the polymer matrix from solutions easier.[32–36] In general, the mechanical strength and stability of polymer matrices can be improved by embedding with nanoparticles. Various techniques have been developed and applied for the preparation of polymer-based nanocomposite. The process of nanocomposite preparation can be generally divided into two parts, i.e. direct compounding and in situ synthesis.[37,38]

In this work, we used water crystallizes as porogens and applied a traditional inverse suspension polymerization technique at subzero temperature. A new method to prepare pAAm-based cryogel beads was also proposed.[13,16,31,32] A direct compounding method was used for the fabrication of a pAAm-based composite cryogel beads with nanoparticles. The functionalization of the pAAm-based cryogel beads were achieved by using the methods reported.[31,36,39]

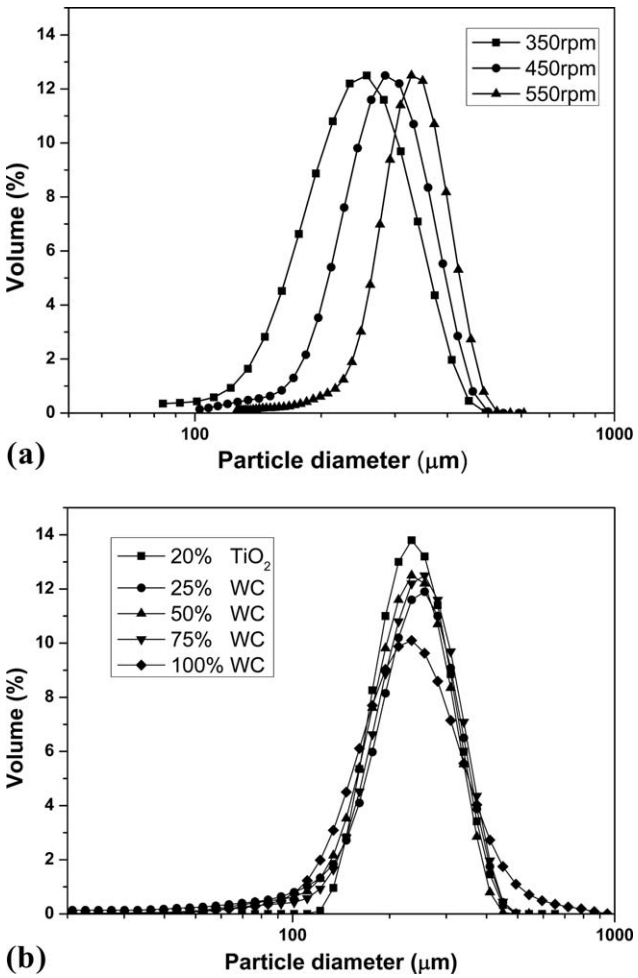

Figure 2. The size distribution of composite beads embedded 20% TiO_2 at different stirring speed (a) and the size distribution of the composite beads embedded different amount of nanoparticles at same stirring speed (b) at −12°C.

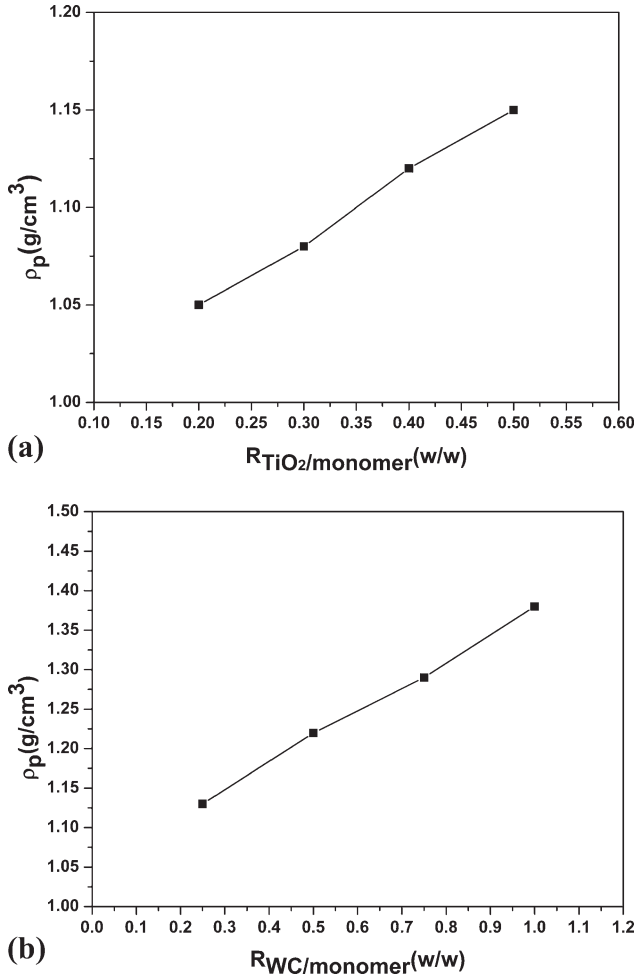

Figure 3. The effect of the addition of nanoparticles on the wet density of superporous beads. (a) The effect of the addition of nano-TiO_2 on the wet density of the superporous beads prepared at −12°C. (b) The effect of the addition of nano-WC on the wet density of the superporous beads prepared at −12°C.

EXPERIMENTS AND METHODS

Materials

Acrylamide (AAm, 99%), *N,N,N′,N′*-tetra-methyl-ethylenediamine(-TEMED, 99%), *N,N′*-methylene-bis(acrylamide)(MBAAm, 99%) and ammonium persulfate (APS, 99%) were supplied by Sigma-Aldrich. TiO_2 (≤25 nm) and WC(tungsten carbide) (≤50 nm) nanoparticles were purchased from DK nano technology (Beijing, China). Other chemicals used were obtained from local sources.

Preparation of Supermacroporous PAAm Cryogel Beads

1.7 g AAm and 0.4 g MBAAm were dissolved in 30 mL deionized water, and then the mixture was degassed under vacuum for 10 min to remove air in the system. The solution was then cooled to 0–5°C, 40 μL TEMED and 200 mg APS were added into the solution to initiate the free radical polymerization. The solution was then added to a glass jar containing 120 g *n*-hexane and 2.4 g Span 80 with mechanical stirring (550 rpm) at 0–5°C. The system was then cooled to T_{prep} (−12°C, −15°C, −18°C) The reaction was stopped after 24 h and the cryogel beads were removed from the organic phase and washed several times with deionized water to remove the unreacted monomers. The beads were subsequently screened with standard sieves of 50–400 μm by wet sieving.

Preparation of Supermacroporous Composite Cryogel Beads with Nanoparticles

The procedure of preparing composite cryogel beads with PAAm and nano-TiO_2 was similar to that of the supermacroporous PAAm cryogel beads. Before adding TEMED and APS to initiate the reaction, nano-TiO_2 was added into the aqueous phase and the mixture was homogenized by sonicating for 30 min at room temperature. TEMED and APS were then added into the mixture to initiate the reaction at 0–5°C. The beads were also screened with standard sieves of 50–400 μm by wet sieving for further characterization.

The amount of nanoparticles was in proportion to the monomers used. The nano-TiO2 used were 20, 30, 40, and 50% of the mass of monomers and the nano-WC used were 25, 50, 75, and 100% of the mass of monomers.

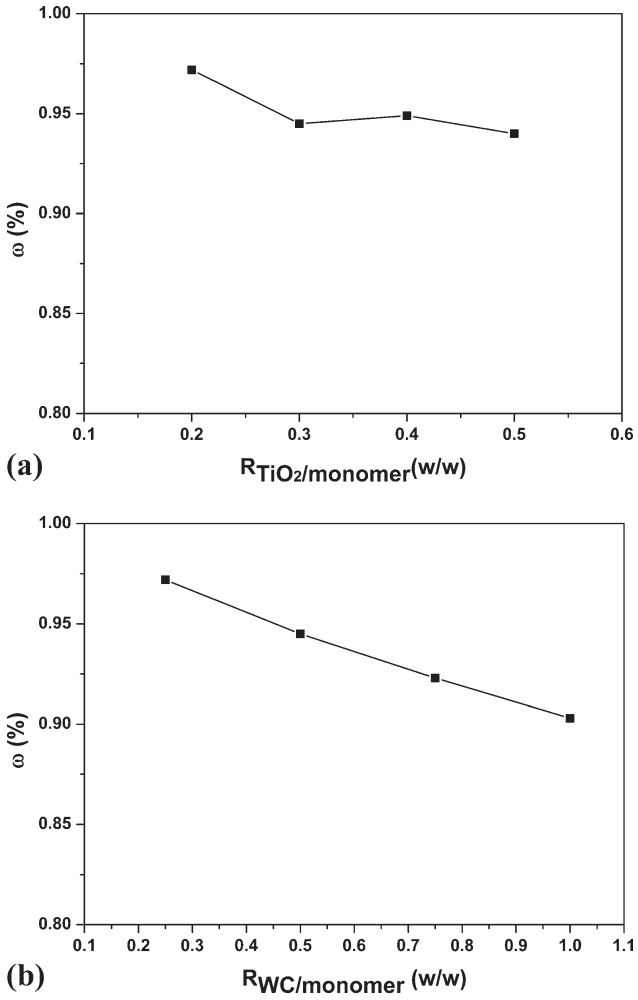

Figure 4. The effect of the addition of nanoparticles on the water content of the beads. (a) The effect of the addition of nano-TiO_2 on the water content of the beads. (b) The effect of the addition of nano-WC on the water content of the beads.

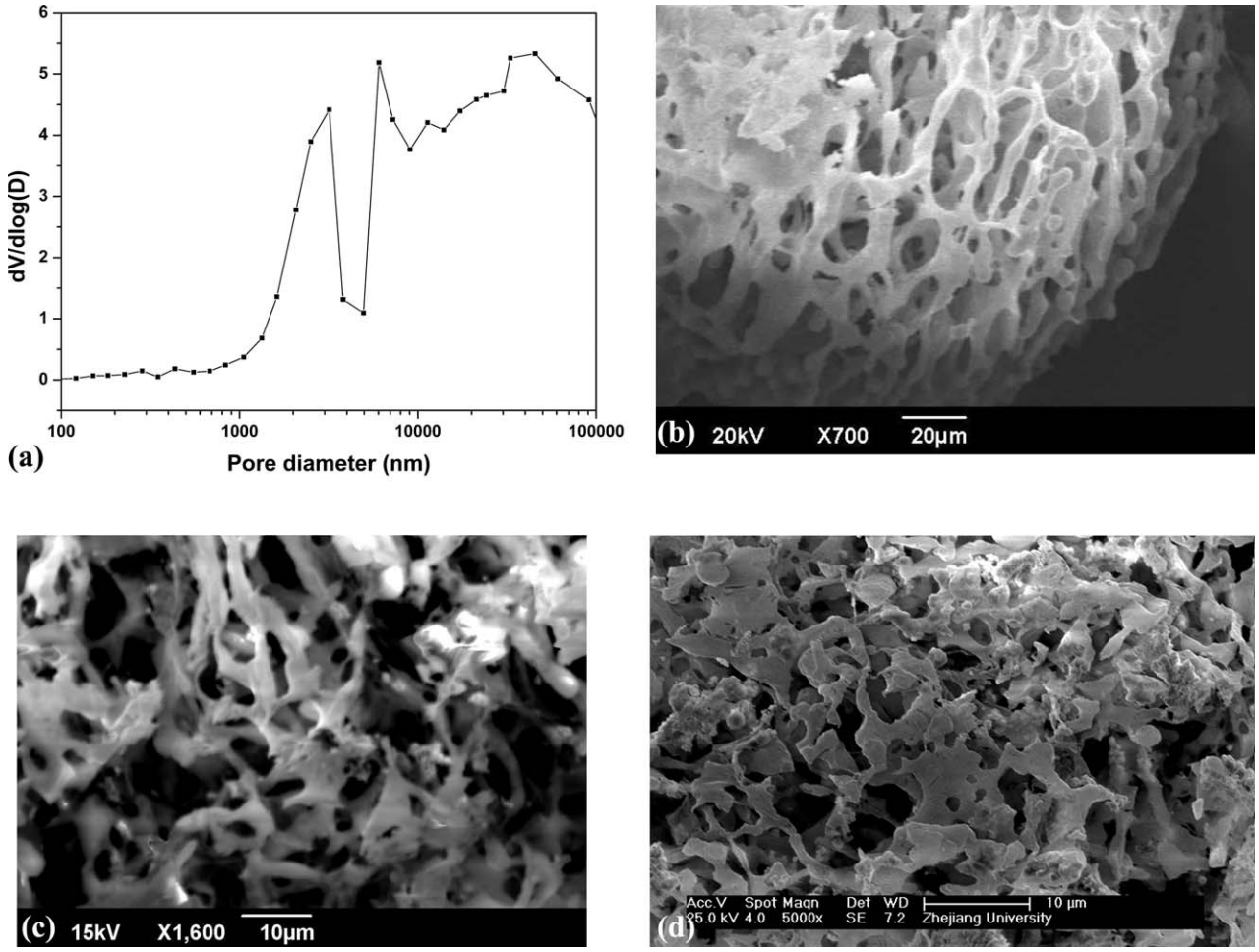

Figure 5. The pore size distribution of the beads and the surface morphologies of the superporous beads embedded with 75% WC prepared at different T_{prep}. (a) The pore size distribution of the superporous beads embedded with 75% nano-WC prepared at −12°C. (b) The surface morphology of the superporous beads prepared at −12°C. (c). The surface morphology of the suerporous beads prepared at −15°C. (d). The surface morphology of the suerporous beads prepared at −18°C.

Characterization of the Supermacroporous PAAm Cryogel Beads

The morphology and structure of the supermacroporous PAAm cryogel beads were studied by scanning electron microscopy (SEM). Samples of the cryogel beads were fixed in 2.5% glutaraldehyde in 0.12 *M* sodium phosphate buffer at pH 7.2 overnight, postfixed in 1% osmium tetroxide for 1 h, dehydrated in ethanol, and the ethanol-dehydrated samples were dried in a critical point dryer (CPD-30) before SEM study according to Ref. 30. The particle size distribution of the beads were measured with Mastersizer 2000 Unit.

Wet density of the beads was measured by water replacement in a 10-mL pycnometer at 25°C. The water content of the beads was measured by drying the samples in a vacuum thermostatic oven at 60°C to a constant mass.

The pore size distribution of the samples was determined by a mercury porosimeter (Quantachrome Corporation, American). The surface area of the dried bead was obtained from N_2 adsorption measurements at −196°C with a NOVA 2000 porosimeter (Quantachrome, American).

To ensure the nanoparticles in the cryogel system, X-ray energy dispersive spectroscopy of the beads was measured by SEM. In our lab, the Ti element dispersive could be measured.

RESULTS AND DISCUSSION

The supermacroporous PAAm cryogel beads were synthesized by inverse suspension polymerization at subzero temperatures and the network was formed by the monomers polymerized in the nonfrozen liquid microphase. Water crystals were formed among the networks as the porogen. The inverse suspension polymerization was a traditional process for the preparation of polymer beads and the morphology of the beads could be adjusted by modifying the procedure. Some important preparation parameters were investigated here, such as reaction temperature, monomers concentration, dispersion system, and cooling control.

The porous structure of the cryogel beads was controlled by the freezing temperature, the concentration of the dissolved monomers, the content of the initiator system, and the solvent used. The preparation temperature as well as the solvent used affected

the porous structure through their effect on the formation of the nonfrozen liquid microphase.[27] In our work, proper concentration of the monomer, the initiator system and the solvent were chosen, therefore the preparation temperature was the main influence factor to the porous structure.

Preparation of the Supermacroporous PAAm Cryogel Beads

Generally, the monomer can be easily dissolved but the time to add the initiator is important. The initiator should be added into the monomer solution before dispersion and the monomer react after dispersion, but the polymerization occurred at the same time when the initiator was added. There was a dispersion process in between so the initiator was added at 0–5°C and the dispersion proceeded at this temperature. Lower temperatures can reduce polymerization rates, therefore the polymerization rate was decreased. The dispersion of the monomer solution in the oil phase was fast and the cooling control was important to form stable inverse suspension system.

The nanoparticles added into the monomer solution would affect the dispersion, therefore the amount of nanoparticles should be controlled. In our experiment, the beads could not be obtained when adding a large amount of nanoparticles.

Morphology and Size Distribution

Figure 1 shows the SEM images of the nonporous beads and the supermacroporous PAAm cryogel beads, which were treated by critical point drying. Figure 1(a) shows that the surface of the nonporous beads was smooth. Figure 1(b) shows that the dried beads have a spherical shape, and there were many irregular supermacropores in the beads. These pores were similar to the cryogel monoliths reported.[28,31] These large pores were originated from the thawing of ice crystal and the size of the pores were up to dozens of micron, the macromolecular solutes can easily pass the pores to the internal area.

Generally, the beads should have a Gaussian size distribution. The size distribution of the swollen cryogel beads were shown in Figure 2. The particle size of the swollen beads showed a logarithmic symmetrical distribution, and the mean sizes of the beads were of 240–330 μm. With the increasing of the stirring speed, the mean diameter of the beads decreased. This result was typical in the preparation of beads with inverse suspension system. With a low stirring speed of below 350 rpm, the dispersion of the AAm solution in the *n*-hexane was inadequate, and the resulting system was instable when the temperature was cooled to T_{prep}. Figure 2(b) shows that at the same stirring speed (550 rpm) at −12°C, the amount of nanoparticles had some impact on the mean diameter of the beads. The results showed that stirring speed was an influence factor of the bead size.

Wet Density and Water Contents

The wet density and the water content were determined under the same method as reported in our previous work.[13,40] Wet density of the beads was determined by water replacement in a 10 mL pycnometer. The free water in the supermacropores of the polymer networks were removed by filtration, only the water combined with the networks retained. The wet densities of the beads with different amounts of nanoparticles were listed

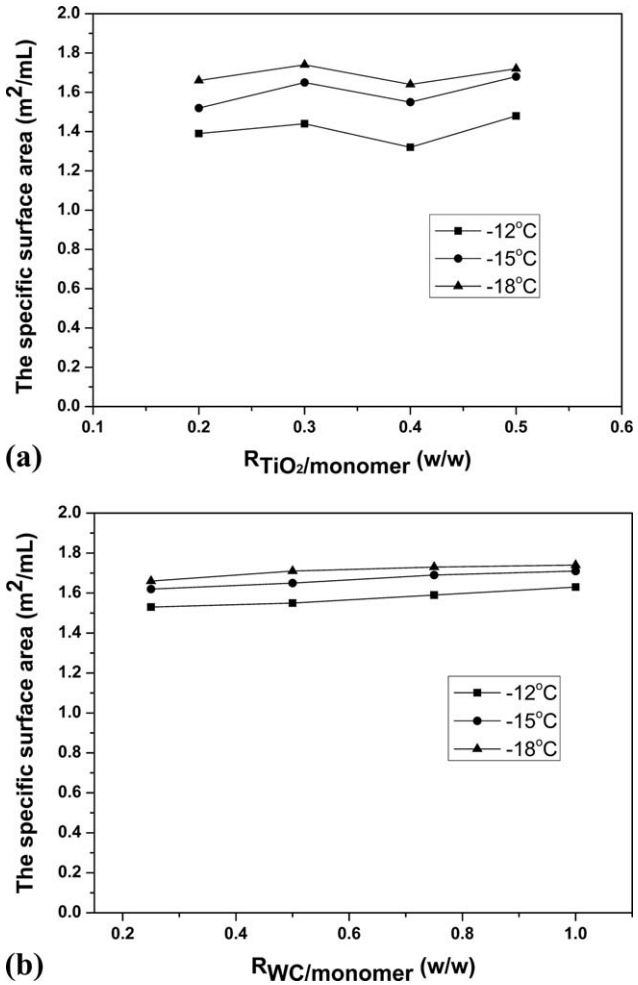

Figure 6. The surface area of surperporous cryogel beads prepared at different conditions. (a) The surface area of addition of nano-TiO_2 at different T_{prep}. (b) The surface area of addition nano-WC at different T_{prep}.

in Figure 3. X Position "*R*" means the weight ratio of nanoparticles to monomers. Moreover, the beads without embedded nanoparticles were also measured and the wet density of these beads was 1.01 g/cm^3, which was closed to the density of water. From the data shown in Figure 3, it was easy to find that with the increase of the nanoparticles, the wet densities of the beads increased as well. When the nanoparticles embedded in the polymer network, some space of the networks was occupied by the nanoparticles. Because of the higher density of the nanoparticles, the density of the combined polymer bead increased. Different nanoparticles had different embedding efficiency. The impact factors mainly include the density, the size and the surface properties of the nanoparticles. Figure 3 shows that by adding same amount of nano-TiO_2 and nano-WC, the density of the beads embedded with nano-WC was much higher, which was because the density of WC was much higher than that of TiO_2.

The water content of the beads was measured by drying the wet samples in a vacuum thermostatic oven at 60°C to a constant weight. The wet samples were filtered to remove the excess water. Figure 4 shows the difference of water content by adding

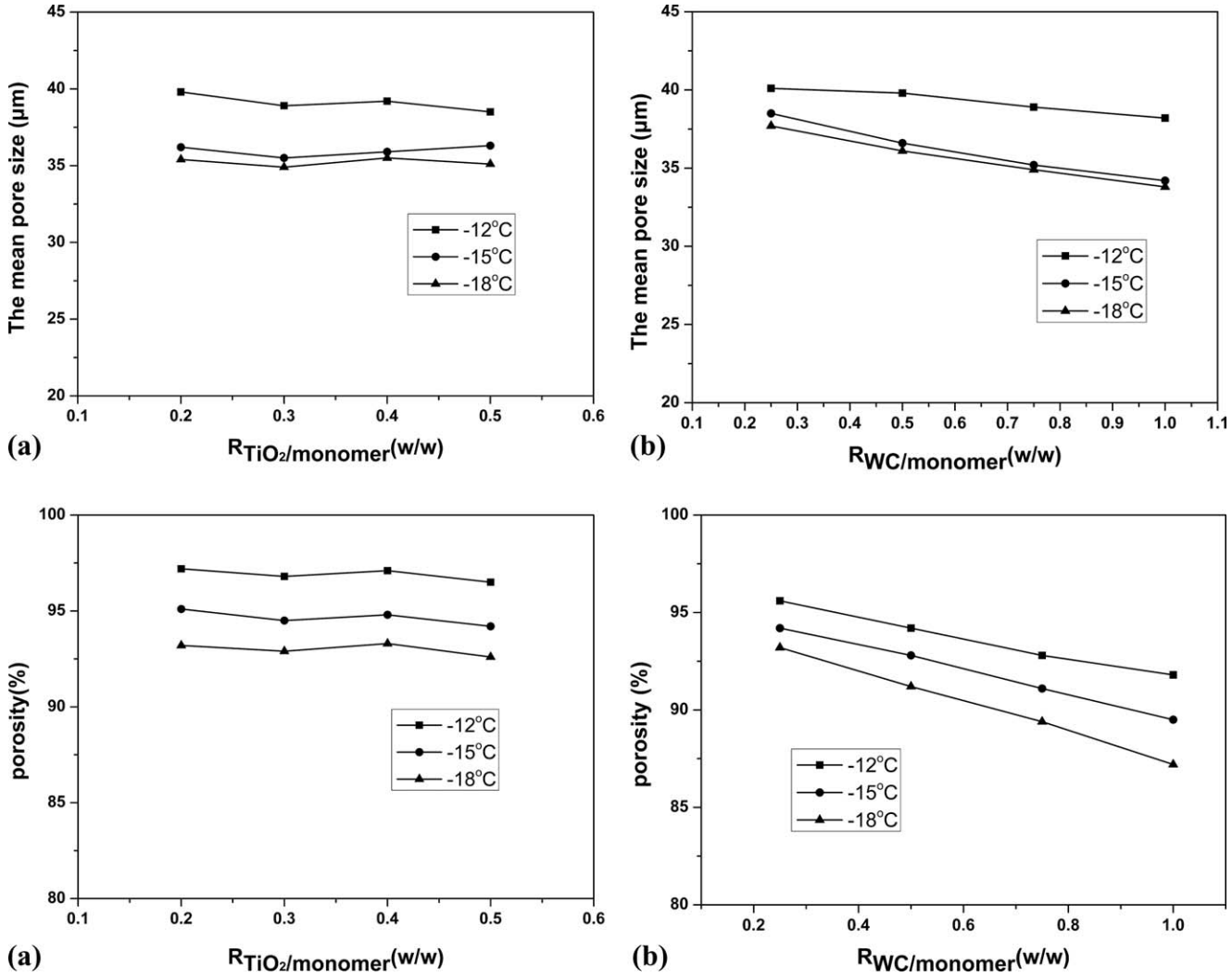

Figure 7. The mean pore size and porosity of the supermacroporous cryogel beads. (a) The mean pore size of nano-TiO_2 embedded at various conditions. (b) The mean pore size of nano-WC embedded at various conditions. (c) The porosity of nano-TiO_2 embedded at various conditions. (d) The porosity of nano-WC embedded at various conditions.

different amount of the nanoparticles to the beads. The results show that, the water content of the composite beads was lower by adding more nanoparticles. The nanoparticle embedded in the polymer networks and occupied the space in the networks which can be filled by water otherwise. Therefore, the water content of the beads was reduced. Such a phenomenon was more obvious when adding nano-WC, because the size of WC ($\leq$50 nm) was much bigger than that of nano-TiO_2 ($\leq$25 nm).

Pore Properties

The pore properties were essential for the applications of porous materials, which influence the effective passage and the binding space in the matrix for target adsorbates.[23,41] The porosity, specific surface area and mean pore size were examined in the study. The effects of nanoparticles and the preparation temperature on the porosity of the beads were the main consideration. Mercury intrusion measurement is a popular method to acquire pore size distribution of porous materials.

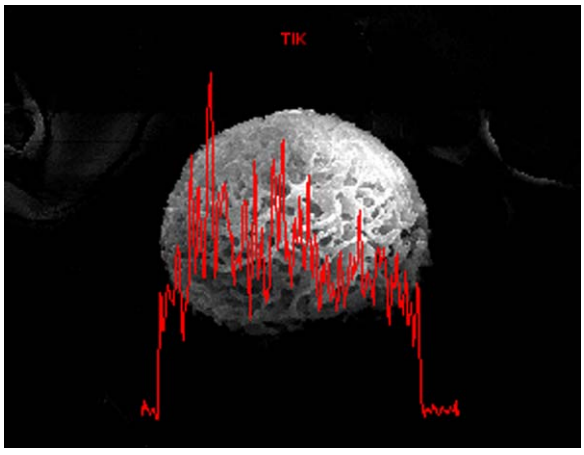

Figure 8. The dispersion of Ti element in cryogel beads embedded with nano-TiO_2. [Color figure can be viewed in the online issue, which is available at wileyonlinelibrary.com.]

The surface areas of the beads were measured from N_2 adsorption at −196°C.[12]

For traditional cryogels, lowering the freezing temperature from −10 to −30°C during the preparation of PAAm cryogels will decrease the flow path properties of these cryogel monoliths and the gelation yield.[26,27]

Figure 5(a) presents the pore size distribution of the supermacroporous beads with 75% nano-WC embedded in the polymer networks. The supermacropores were of 3–100 μm, and the mean pore size was 35 μm. Figure 5(b–d) were the surface morphology of the beads prepared at different T_{prep}. The beads prepared at different T_{prep} had similar supermacroporous surface morphology. The pore sizes of these beads were all in the range of several to dozens of micrometers, and the beads prepared at −12°C had the maximum the pore size. The supermacropores made the beads suitable for various biochemical applications, especially for the extraction of effective components from solutions containing small solid particles. These results were similar to the traditional cryogels. The difference in pore structure of the cryogels prepared at −12 or −18°C, respectively, was a result of different cooling rates. The samples appeared to be frozen at −18°C within 4–6 min, while in took 12–15 min at −12°C.[42]

The specific surface area and the mean pore size of the composite beads are shown in Figures 6 and 7. For all preparation conditions, the beads prepared at −12°C showed the biggest mean pore size and the lowest specific surface area. Addition of different amount of the nanoparticles had few effects on the specific surface area and the mean pore size.

The surface area of the dried beads was acquired from N_2 adsorption measurements at −196°C. Figure 6 shows that the amount of nanoparticles adding into the cryogel beads networks had few effects on the specific surface area. The beads prepared at −12°C had the lowest specific surface area. The specific surface areas were among 1–2 m^2/mL which was low because of the supermacropores and the high porosity.

The mean pore size and the porosity were measured by a mercury porosimeter. The result in Figure 7 shows that the beads prepared at higher T_{prep} had a bigger mean pore size and higher porosity. And the porosity of the beads embedded with nanoparticles reduced while the amount of the nanoparticles raised. Generally, these results are consistent with the result of the water content and the specific surface area measured. The mean pore size of the beads was higher than 20 μm, which can used in a wide range of applications.

Energy Dispersive Spectrometer of the Cryogel Beads

The dispersion of Ti element was measured by Energy Dispersive Spectrometer. The result in Figure 8 shows that Ti element dispersed in the area of the beads much higher than the environment, so the nano-TiO_2 successfully embedded into the beads.

CONCLUSIONS

PAAm-based cryogel beads can be prepared by cooling the inverse suspension polymerization system to subzero temperatures. The free-radical polymerization was happened in the unfrozen liquid microphase to form polymer networks while the water crystallized can be used as the porogen. The nanoparticles embedded cryogel beads can also be fabricated by the same procedure. The size distribution and the mean diameter of the cryogel beads were depend on the ratio of the aqueous phase to the water-immiscible phase and also the stirring speed. These cryogel beads showed a supermacroporous interconnected structure, high swelling kinetics, and proper mechanical properties. The size of the beads were of 50–400 μm and the distribution of the beads showed a normal distribution. The beads had large pores of 3–90 μm in diameter and the porosity of the beads can be up to 90%. Comparing to the traditional porous beads, the cryogel beads can allow the macromolecules easily pass through because of its supermacroporous structures. The beads prepared had good water absorption capability faster water adsorption rate. All these properties show that the beads prepared are suitable for biochemical applications, such as support for catalysts, immobilization of enzymes and cells, adsorptions, release of active substances, and so forth ms. The supermacroporous cryogel beads expanded the scopes of the PAAm-based beads, for the cryogel beads had supermacropores of 3–90 μm. The composite cryogel beads with nanoparticles also expanded the application of these beads.

ACKNOWLEDGMENTS

This work was supported by National Natural Science Foundation of China.

REFERENCES

1. Park, J.; Kim, Y.; Yoon, H.; Jun, B.; Lee, Y. *J. Ind. Eng. Chem.* **2011**, *17*, 794.
2. Dukić-Ott, A.; Thommes, M.; Remon, J. P.; Kleinebudde, P.; Vervaet, C. *Eur. J. Pharm. Biopharm.* **2009**, *71*, 38.
3. Li, X.; Li, Y.; Ye, Z. *Chem. Eng. J.* **2011**, *178*, 60.
4. Rämö, V.; Anghelescu-Hakala, A.; Nurmi, L.; Mehtiö, T.; Salomäki, E.; Härkönen, M.; Harlin, A. *Eur. Polym. J.* **2012**, *48*, 1495.
5. Liu, C.; Wei, N.; Wang, S.; Xu, Y. *Carbohydr. Polym.* **2009**, *78*, 1.
6. Gustavsson, P.; Larsson, P. *J. Chromatogr. A* **1996**, *734*, 231.
7. Yang, Y.; Nam, S.; Lee, N. Y.; Kim, Y. S.; Park, S. *Ultramicroscopy* **2008**, *108*, 1384.
8. Gümüşderelioğlu, M.; Erce, D.; Demirtaş, T. *J. Mater. Sci. Mater. Med.* **2011**, *22*, 2467.
9. Choi, S.; Zhang, Y.; Yeh, Y.; Wooten, A. L.; Xia, Y. *J. Mater. Chem.* **2012**, *22*, 11442.
10. Kale, S.; Lali, A. *Biotechnol. Prog.* **2011**, *27*, 1078.
11. Shi, Q.; Zhou, X.; Sun, Y. *Biotechnol. Bioeng.* **2005**, *92*, 643.
12. Wang, D.; Hao, G.; Shi, Q.; Sun, Y. *Chromatogr. A* **2007**, *1146*, 32.
13. Shi, F.; Lin, D.; Phottraithip, W.; Yao, S. *J. Appl. Polym. Sci.* **2011**, *119*, 3453.
14. Li, H.; Cui, X.; Shen, S.; Hu, D. *J. Appl. Polym. Sci.* **2011**, *122*, 509.

15. Wu, S.; Liou, T.; Yeh, C.; Mi, F.; Lin, T. *J. Appl. Polym. Sci.* **2013**, *127*, 4573.
16. Phottraithip, W.; Lin, D.; Shi, F.; Yao, S. *J. Appl. Polym. Sci.* **2011**, *121*, 2985.
17. Erzengin, M.; Ünlü, N.; Odabaşı, M. *J. Chromatogr. A* **2011**, *1218*, 484.
18. Plieva, F. M.; Galaev, I. Y.; Noppe, W.; Mattiasson, B. *Trends Microbiol.* **2008**, *16*, 543.
19. He, X.; Yao, K.; Shen, S.; Yun, J. *Chem. Eng. Sci.* **2007**, *62*, 1334.
20. Kathuria, N.; Tripathi, A.; Kar, K. K.; Kumar, A. *Acta Biomater.* **2009**, *5*, 406.
21. Ceylan, D.; Ozmen, M. M.; Okay, O. *J. Appl. Polym. Sci.* **2006**, *99*, 319.
22. Kuyukina, M. S.; Rubtsova, E. V.; Ivshina, I. B.; Ivanov, R. V.; Lozinsky, V. I. *J. Microbiol. Methods* **2009**, *79*, 76.
23. Plieva, F. M.; Karlsson, M.; Aguilar, M.; Gomez, D.; Mikhalovsky, S.; Galaev, I. Y.; Mattiasson, B. *J. Appl. Polym. Sci.* **2006**, *100*, 1057.
24. Lozinsky, V. I.; Galaev, I. Y.; Plieva, F. M.; Savina, I. N.; Jungvid, H.; Mattiasson, B. *Trends Biotechnol.* **2003**, *21*, 445.
25. Yun, J.; Kirsebom, H.; Galaev, I. Y.; Mattiasson, B. *J. Sep. Sci.* **2009**, *32*, 2601.
26. Lozinsky, V. I.; Plieva, F. M.; Galaev, I. Y.; Mattiasson, B. *Bioseparation* **2001**, *10*, 163.
27. Plieva, F. M.; Galaev, I. Y.; Mattiasson, B. *J. Sep. Sci.* **2007**, *30*, 1657.
28. Lozinsky, V. I. *Russ. Chem. Rev.* **2002**, *71*, 489.
29. Plieva, F. M.; Seta, E. D.; Galaev, I. Y.; Mattiasson, B. *Sep. Purif. Technol.* **2009**, *65*, 110.
30. Demiryas, N.; Tüzmen, N.; Galaev, I. Y.; Pişkin, E.; Denizli, A. *J. Appl. Polym. Sci.* **2007**, *105*, 1808.
31. Yun, J.; Tu, C.; Lin, D.; Xu, L.; Guo, Y.; Shen, S.; Zhang, S.; Yao, K.; Guan, Y.; Yao, S. *J. Chromatogr. A* **2012**, *1247*, 81.
32. Zhao, X.; Lv, L.; Pan, B.; Zhang, W.; Zhang, S.; Zhang, Q. *Chem. Eng. J.* **2011**, *170*, 381.
33. Yang, D.; Li, J.; Jiang, Z.; Lu, L.; Chen, X. *Chem. Eng. Sci.* **2009**, *64*, 3130.
34. Mohamed, A. E. R.; Rohani, S. *Energy Environ. Sci.* **2011**, *4*, 1065.
35. Sahle-Demessie, E.; Tadesse, H. *Surf. Sci.* **2011**, *605*, 1177.
36. Yao, K.; Shen, S.; Yun, J.; Wang, L.; Chen, F.; Yu, X. *Biochem. Eng. J.* **2007**, *36*, 139.
37. Seo, Y. G.; Woo, K.; Kim, J.; Lee, H.; Lee, W. *Adv. Funct. Mater.* **2011**, *21*, 3094.
38. Tong, Y.; Li, Y.; Xie, F.; Ding, M. *Polym. Int.* **2000**, *49*, 1543.
39. Yun, J.; Shen, S.; Chen, F.; Yao, K. *J. Chromatogr. B* **2007**, *860*, 57.
40. Xia, H.; Lin, D.; Yao, S. *J. Chromatogr. A* **2007**, *1175*, 55.
41. Kostova, B.; Momekova, D.; Petrov, P.; Momekov, G.; Toncheva-Moncheva, N.; Tsvetanov, C. B.; Lambov, N. *Polymer* **2011**, *52*, 1217.
42. Plieva, F. M.; Savina, I. N.; Deraz, S.; Andersson, J.; Galaev, I. Y.; Mattiasson, B. *J. Chromatogr. B* **2004**, *807*, 129.